Available online at www.sciencedirect.com
ScienceDirect
Biochemical and Biophysical Research Communications 360 (2007) 103–108
BBRC
www.elsevier.com/locate/ybbrc

The NMR solution structure of recombinant RGD-hirudin ☆,☆☆

Xia Song [a], Wei Mo [b], Xingang Liu [a], Lina Zhu [a], Xiaomin Yan [a], Houyan Song [b,*], Linsen Dai [a,*]

[a] *Center of Analysis and Measurement, Fudan University, Shanghai 200433, China*
[b] *Key Laboratory of Molecular Medicine, Ministry of Education, Fudan University, Shanghai 200032, China*

Received 31 May 2007
Available online 13 June 2007

Abstract

The solution structure of a new recombinant RGD-hirudin, which has the activities of anti-thrombin and anti-platelet aggregation, was determined by ^{1}H nuclear magnetic resonance spectroscopy and compared with the conformations of recombinant wild-type hirudin and hirudin (variant 2, Lys47) of the hirudin thrombin complex. On the basis of total 1284 distance and dihedral angle constraints derived from a series of NMR spectra, 20 conformers were computed with ARIA/CNS programs. The structure of residues 3–30 and 37–48 form a molecular core with two antiparallel β-sheets as the other two hirudins. However, significant differences were found in the surface electrostatic charge distributions among the three hirudins, especially in the RGD segment of recombinant RGD-hirudin. This difference may be greatly beneficial to its additional function of anti-platelet aggregation. The difference in extended C-terminal makes its both ionic and hydrophobic interactions with the fibrinogen recognition exosite of thrombin more effective.
© 2007 Elsevier Inc. All rights reserved.

Keywords: Recombinant RGD-hirudin; NMR; Solution structure; Electrostatic surface

In our laboratory, a new type of recombinant RGD-hirudin has been successfully cloned, expressed in the methylotrophic yeast *Pichia pastoris* and consequently purified [1]. By active assay, it has been proved that the recombinant RGD-hirudin not only has a specific activity of 12,000 ATU mg^{-1}, but also shows the dual function of anti-thrombin and anti-platelet aggregation. As a comparison, the wild-type hirudin only has the former function. In our previous work, a series of two-dimensional ^{1}H NMR spectra and resonance assignment of recombinant RGD-hirudin were presented in our previous paper [2]. To establish a more direct correlation between the additional anti-platelet aggregation function and its structure, we calculated the three-dimensional structure of recombinant RGD-hirudin based on the 1284 distance restraints and torsion angle restraints derived from NMR measurements. We executed our calculation on the ARIA [3–7] version 2.0, and CNS [8] version 1.1 programs. The results were compared with the previously reported conformations of recombinant wild-type hirudin and hirudin (variant 2, Lys47) of the hirudin thrombin complex (which is represented as hirudin (variant 2, Lys47) in the following) [9,10]. It is beneficial to explain the relative effectiveness and additional anti-platelet aggregation function of the recombinant RGD-hirudin.

Abbreviations: NMR, nuclear magnetic resonance; RMSD, average root-mean square deviation; NOE, nuclear overhauser effect; ARIA, ambiguous restraints in iterative assignment; CNS, Crystallography and NMR System; FRE, fibrinogen recognition exosite.

☆ Contract/grant sponsor: Youth Foundation of Fudan University and Foundation of Important Science and Technology Key Items of Shanghai Science and Technology Committee; Contract/Grant No.: 034319203.

☆☆ These institutes (Center of Analysis and Measurement, Fudan University, Shanghai 200433, China and Key Laboratory of Molecular Medicine, Ministry of Education, Fudan University, Shanghai 200032, China) contributed equally to this work.

* Corresponding authors.
E-mail addresses: hysong@shmu.edu.cn (H. Song), lsdai@fudan.edu.cn (L. Dai).

0006-291X/$ - see front matter © 2007 Elsevier Inc. All rights reserved.
doi:10.1016/j.bbrc.2007.06.014

Materials and methods

The recombinant RGD-hirudin was provided by one of the authors (H.S.) [1]. All NMR spectra were recorded on a Bruker DMX500 spectrometer equipped with pulsed Z-gradients at 25 °C. NMR data processing and analysis were carried out using Bruker XWIN-NMR and Sparky software [2].

The ARIA [3–7] version 2.0 and CNS [8] version 1.1 programs were employed to calculate the solution structure. All NOE cross-peaks were from three NOESY spectra with mixing time 50, 100, and 150 ms. Finally, 1208 distances were obtained using the standard r^{-6} dependence of the NOE volumes. In addition, 26 distance restraints for 13 backbone NH(i)–CO(j) hydrogen bonds were identified according to the criteria laid out by Wagner et al. [11]. Nine distance restraints were included to define three disulfide bridges between Cys6 and Cys14, Cys16 and Cys28, Cys22 and Cys39 [12]. A total of 26 Φ backbone torsion angle restraints were derived from $^{3}J_{HN\alpha}$ coupling constants measured from the DQF-COSY spectra in H_2O [13]. A total of 15 χ_1 side-chain torsion angle restraints were derived from the COSY spectra in H_2O based on the $^{3}J_{\alpha\beta}$ coupling constants, and from the relative intensities of the NH–C^{β}H and C^{α}H–C^{β}H NOES in the NOESY spectra [12].

Finally, 600 structures were calculated and the ensemble of the 20 structures *refined in water* were deposited in PDB (ID 2JOO) and RCSB (ID RCSB100096).

Results

Resonance assignment

Spectral assignments and reference data had been published in our previous paper [2]. However, during our further analysis of the NMR spectra for structure calculation, we realized that some previous resonance assignments needed to be corrected. They are the chemical shifts of Tyr3 δH (6.93–7.05 ppm), Tyr3 εH (6.55–6.67 ppm), Ile 29 γCH_2 (1.54, 1.33–1.54, 1.42 ppm), Lys36 βH (1.87, 1.87–2.01, 1.97 ppm), Lys36 γCH_2 (2.01, 1.97–1.85, 1.87 ppm), Tyr64 δH (7.02–6.93 ppm), Tyr64 εH (6.71–6.55 ppm).

Structure calculation

The mean structure (shown in Fig. 1A) and the 20 structures ensemble were displayed and analyzed using MOLMOL [14] and PROCHECK [15,16]. It is clear that the conformation of the N-terminal core formed by residues 3–30 and 37–48 was well determined. The RMSDs of this core between the individual structures and the mean structure were 0.50 ± 0.13 Å for backbone atoms and 1.02 ± 0.15 Å for all heavy atoms respectively. In contrast, neither the conformation of the C-terminal polypeptide segment 49–66 nor its orientation relative to the other parts of the molecule was defined by the NMR data, as well as the loop formed by residues 31–36.

The core formed by residues 3–30 and 37–48 was principally stabilized by the three disulfide bridges between Cys6 and Cys14, Cys16 and Cys28, Cys22 and Cys39. The 1–5 residues formed an irregular strand which led into a loop closed off at its base by the disulfide bridge between Cys6 and Cys14. Residues 5–8 formed a typical half-turn and segment 8–11 formed a typical type II turn, followed by a mini-antiparallel β-sheet formed by residues 14–16 (strand I) and 21–23 (strand I′). The two β-strands were connected by a type II tight turn (residues 17–20). On the other hand, strand I′ led to the second antiparallel β-sheet formed by residues 26–30 (strand II) and 37–41 (strand II′) connected by a β-turn (residues 32–35). Finally, strand II′ led into an irregular strand which folded back onto the protein such that residue Lys47 was in close proximity to residues that were closed off by the disulfide bridge between Cys6 and Cys14. Residues 31–36 form an exposed finger of antiparallel β-sheet, whose orientation with respect to the core could not be determined on the basis of the present data. This was due to the fact that no long-range NOEs from residues 31–36 to the core could be detected. The large local RMSDs for the backbone atoms and the large ranges of values for the backbone dihedral angles of residues of 31–36 showed that the increased disorder could not simply be attributed to a hinge motion.

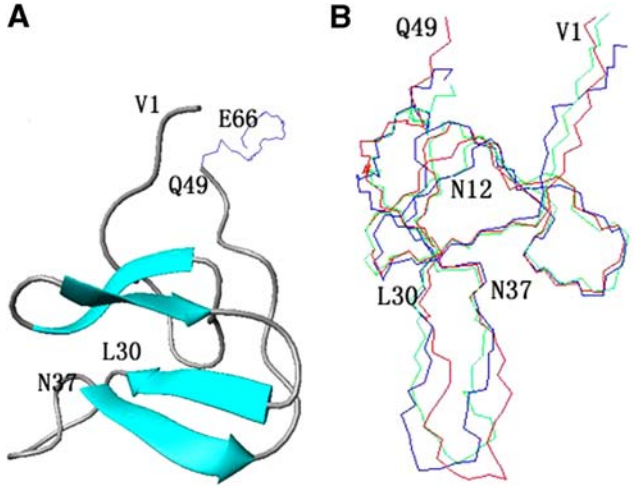

Fig. 1. (A) Schematic ribbon drawing of recombinant RGD-hirudin from residue 1 to residue 66. The arrowed ribbons indicate the position and direction of the β-sheet strands. (B) Stereo view of the polypeptide backbone of the mean structure of recombinant RGD-hirudin (1–49, in blue), the corresponding 49 residues segments of recombinant wild-type hirudin (in green) and hirudin (variant 2, Lys47) of the hirudin thrombin complex (in red). The three structures were superimposed for the backbone atoms of residues 3–30 and 37–48. (*In order to compare the hirudin structures [9,10] conveniently, residues 1–49 was taken as hirudin.) (For interpretation of the references in color in this figure legend, the reader is referred to the web version of this article.)

Analysis of the ensemble of 20 structures by PROCHECK [15,16] revealed that, 72.7% and 26.8% residues lay in the most favored or additionally allowed regions of Ramachandran plot, respectively. Of the remaining, 0.4% and 0.1% residues located in the generously allowed and disallowed regions, respectively.

Discussion

The recombinant RGD-hirudin was constructed by introducing the Arg-Gly-Asp (RGD) sequence replacing the sequence of Ser-Asp-Gly (residues 32–34) in wild-type

hirudin. It was also constructed by some changes to the C-terminal by employing recombinant DNA technique. In order to compare the structure of recombinant RGD-hirudin with that of recombinant wild-type hirudin [9] and with the hirudin (variant 2, Lys47) [10], the three structures were superimposed for the backbone atoms of residues 3–30 and 37–48 (shown in Fig. 1B). It was shown that the conformations of residues 3–30 and 37–48 of the well-defined protein cores were nearly identical in the three molecules. The segments of residues 31–36 were not uniquely defined and appeared to be largely disordered within the three molecules. Local conformational differences were identified for the polypeptide segments 1–3, 11–13 and 48–49 mainly.

A more detailed comparison of the structures of recombinant RGD-hirudin, recombinant wild-type hirudin [9] and hirudin (variant 2, Lys47) [10] is presented in Fig. 2. The first two residues in segment 1–6 were not well defined mainly due to the small number of NOE restraints. The orientation of the aromatic ring of Tyr 3 about the dihedral angle χ_2 was disordered and appeared differently in the three hirudins. This effect originated mainly from the use of pseudoatoms for the ring protons, which was inevitable because of the chemical shift degeneracy of the symmetry-related ring protons. The segment 7–11 was well defined except for the side chain of Glu8. For the next well defined segment 12–16, the only difference was on the side chain of

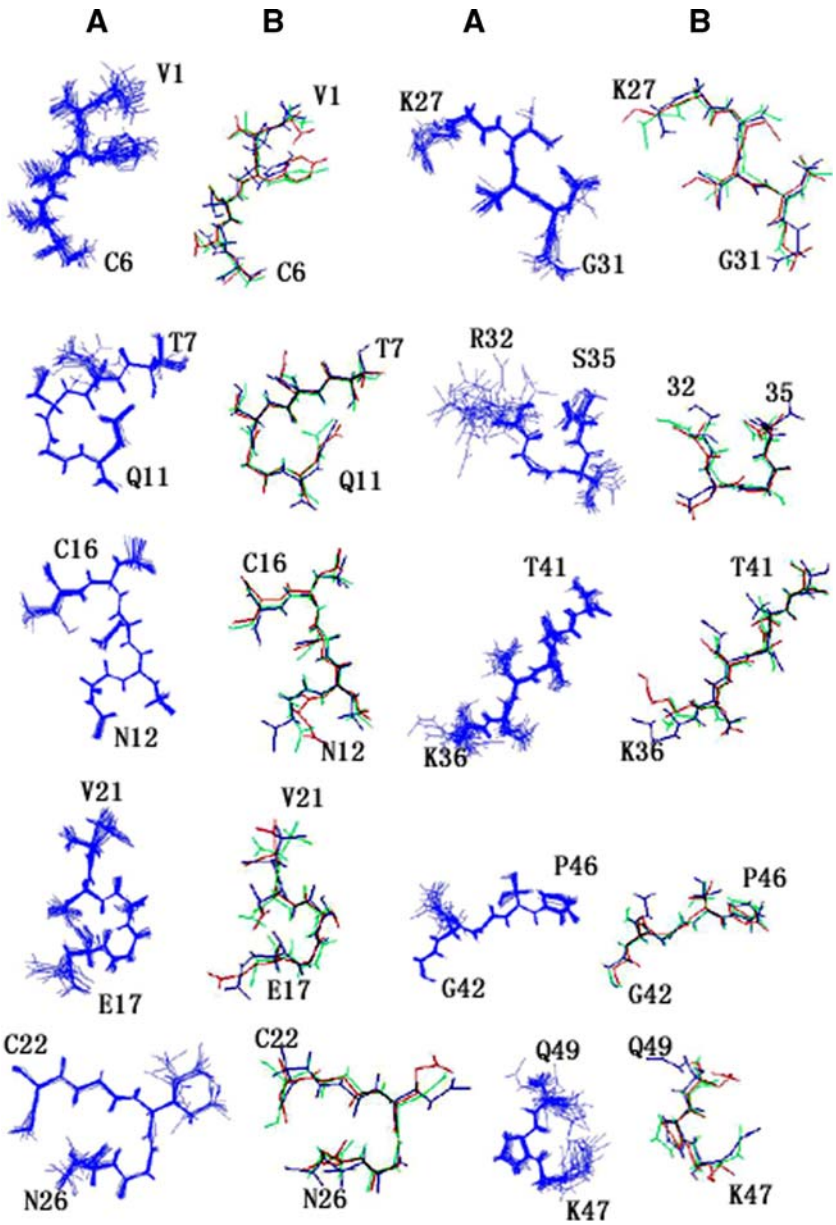

Fig. 2. (A) Stereo pictures of individual segments of all heavy atoms representation of the ensemble of 20 conformers of recombinant RGD hirudin (1–49). (B) Stereo pictures of individual segments of all heavy atoms representation of the mean structure of recombinant RGD hirudin (blue), recombinant wild-type hirudin (green) and hirudin (variant 2, Lys47) (red). All the segments were superimposed for the backbone atoms of the individuals. (For interpretation of the references in color in this figure legend, the reader is referred to the web version of this article.)

Asn12 in the three hirudins. In the segments 17–21 and 22–26, local disorder prevailed for the side chain of Glu17, Gln24 and Asn26. The β-strands of residues 14–16 (strand I) and 21–23 (strand I′) were connected by a type II tight turn (residues 17–20). The segment 27–31 was well ordered except for the side chains of Lys27. On the other hand, for a few of the 20 conformations, the side chains of Cys28 and Ile29 were rotated away from the orientation in the ensemble. In the segment 36–41, the side chains of the first three residues were noticeably disordered, but residues 39–41 were well defined. The disorder of Lys36 occurred mainly because of the incomplete assignment of its long side chain and shortage of relative NOE restraints. The second antiparallel β-sheet was composed of residues 26–30 (strand II) and 37–41 (strand II′), which were connected by a type I′ turn between residues 32 and 35. In spite of the different global orientations of this loop in the ensemble group, the local fit was good, except for the disorder of the long chain of Lys32. It happened for the same reason as in Lys36. Nonetheless, most of the backbone dihedral angles of residues 31–37 had relatively large variability so that the appearance of two groups of 20 conformers could not be entirely attributed to a localized hinge motion at residues 31 and 36. In segments 42–46 and 47–49, only the side chains of Glu43, Lys47 and Gln49 were poorly constrained. The important interaction sites Pro46 and Pro48 were well defined for both backbone and side chains, and basically agreed with the conformations of recombinant wild-type hirudin and hirudin (variant 2, Lys47).

The conformation of the N-terminal core of recombinant RGD-hirudin formed by residues 3–30 and 37–48 was principally stabilized by the three disulfide bridges between Cys6 and Cys14, Cys16 and Cys28, and Cys22 and Cys39. The disulfide bonds of Cys6–Cys14 and Cys16–Cys28 were nearly perpendicular, while Cys16–Cys28 and Cys22–Cys39 were nearly parallel, which was similar with hirudin (variant 2, Lys47). A list of the sulfur–sulfur distances in the structures of recombinant RGD-hirudin, recombinant wild-type hirudin [9] and hirudin (variant 2, Lys47) [10] is given in Table 1. From the table, it is clear that the sulfur–sulfur distances of recombinant RGD-hirudin and in hirudin (variant 2, Lys47) are more similar except for those of Cys6–Cys39, Cys16–Cys39 and Cys28–Cys39, which have deviation values of 1.42 Å, 2.07 Å, and 1.04 Å, respectively.

Thrombin is a serine protease that plays a central role in blood coagulation. However, its function can be inhibited by hirudin. Structural studies conducted on hirudin in the free [9,17–21] and thrombin-bounded state [10,22] indicated that the C-terminal of hirudin also plays an important role in the interaction with thrombin, such as its long extended conformation interacts with a multitude of residues on the thrombin surface. This cliff-like binding exosite of thrombin is an extension of the active-site-cleft and it is particularly abundant in positively charged side chains of the Phe34 to Leu41 and Lys70 to Glu80 loops of thrombin [23]. In the C-terminal of the recombinant

Table 1
Sulfur–sulfur distances in the recombinant RGD-hirudin, recombinant wild-type hirudin and hirudin (variant 2, Lys47)

	Recombinant RGD-hirudin (Å)	Recombinant wide-type (Å)	Hirudin (variant 2, Lys47) (Å)
Cys6–Cys14	2.83	2.02	2.01
Cys6–Cys16	4.07	3.73	4.72
Cys6–Cys22	6.90	7.85	6.11
Cys6–Cys28	3.29	5.58	3.74
Cys6–Cys39	6.23	7.93	7.65
Cys14–Cys16	6.41	3.44	6.43
Cys14–Cys22	7.30	7.03	6.56
Cys14–Cys28	5.35	5.09	5.43
Cys14–Cys39	7.68	7.59	8.32
Cys16–Cys22	5.26	4.21	4.70
Cys16–Cys28	2.40	2.02	2.06
Cys16–Cys39	3.15	4.40	5.22
Cys22–Cys28	5.82	3.05	5.48
Cys22–Cys39	2.74	2.02	2.05
Cys28–Cys39	4.54	3.60	5.58

wild-type hirudin [9] and hirudin (variant 2, Lys47) [10], there were six negatively charged residues: Asp53, Asp55, Glu57, Glu58, Glu61 and Glu62. While in the recombinant RGD-hirudin, we altered the charged distribution of the C-terminal by employing recombinant DNA technique. They are Asp55, Glu57, Glu61, Asp62 and Asp65 and Glu66, respectively. We mutated Glu62 and Gln65 to

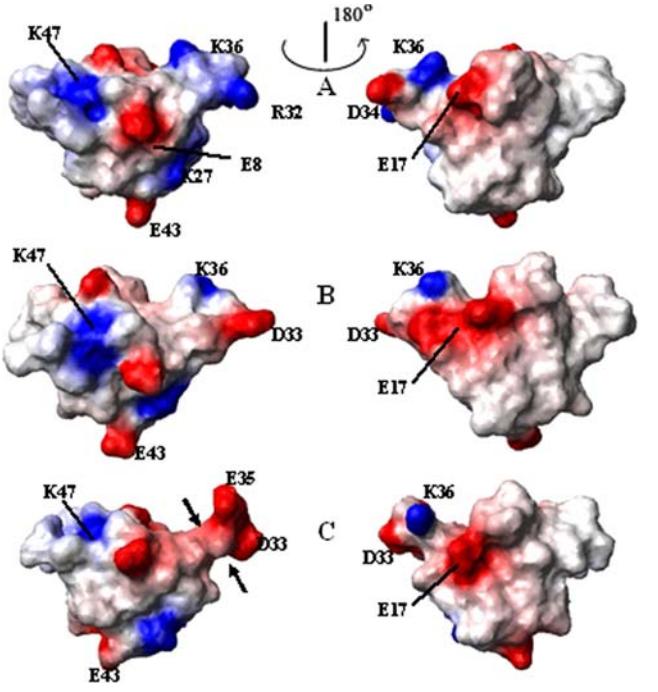

Fig. 3. Electrostatic surfaces of the structures (1–49) of (A) recombinant RGD-hirudin, (B) recombinant wild-type hirudin and (C) hirudin in the X-ray complex crystal structure. Red, negative; blue, positive. (For interpretation of the references in color in this figure legend, the reader is referred to the web version of this article.)

negatively charged residues of Asp62 and Asp65. We also mutated Asp53 and Glu58 to Gln53 and Pro58 as well as added Glu66. These changes improved its hydrophobicity and made the recombinant RGD-hirudin interact more effectively with the fibrinogen recognition exosite of thrombin, resulting in a specific activity of 12,000 ATU mg^{-1} [1].

Fig. 3 shows the electrostatic surfaces of the structures (1–49) of recombinant RGD-hirudin, recombinant wild-type hirudin and hirudin (variant 2, Lys47), respectively. Although most of the surface charge distributions are identical in the three structures, such as the negatively charged patches Glu8, Glu17 and Glu43, and the positively charged patch Lys27, the location of positively charged patch Lys47 in hirudin (variant 2, Lys47) has a little change. There is also a great difference in the loop of 32–35. The electrostatic surface shape of the segment 32–35 in hirudin (variant 2, Lys47) (Fig. 3C) is obviously narrower than both NMR structures, which is the result of interaction between hirudin thrombin complex. Owing to the mutation of the segment 32–35, the positively charged patch Arg32 and negatively charged patch Asp34 in the recombinant RGD-hirudin differ greatly from the two negatively charged patches of Asp33 and Glu35 in recombinant wild-type hirudin and hirudin (variant 2, Lys47). This mutated segment can bind to integrin receptor GPIIb/IIIa, so the recombinant RGD-hirudin could efficiently inhibit fibrinogen-mediated platelet cell aggregation. The assay [1] showed that the rate of anti-platelet aggregation reaches 100 when using 0.008 mg ml^{-1} of recombinant RGD-hirudin, whereas there was no function of anti-platelet aggregation for wild-type hirudin. This additional function is mainly due to the segment of RGD.

To conclude, recombinant RGD-hirudin has the dual function of anti-thrombin and anti-platelet aggregation, making it a good candidate for various clinical applications. To further investigate the structure–function relationships of the recombinant RGD-hirudin, various experiments and calculations are being conducted in our laboratory now.

Acknowledgments

We thank Professor Liping Wang and Tailiu Wu (Center of Analysis And Measurement, Fudan University, Shanghai, China) for providing measurement time on the DMX500 spectrometer and discussions of the NMR experiments. This study was supported by the Youth Foundation of Fudan University, Shanghai, and the Foundation of Important Science and Technology Key Items of Shanghai Science and Technology Committee (034319203).

Appendix A. Supplementary data

Supplementary data associated with this article can be found, in the online version, at doi:10.1016/j.bbrc.2007.06.014.

References

[1] W. Mo, Y. Zhang, L. Wang, X. Yang, H. Song, Fermentation, purification and identification of recombinant RGD-hirudin, Chin. J. Biotechnol. 20 (2004) 126–129.
[2] X. Liu, X. Yan, W. Mo, H. Song, L. Dai, ^{1} H NMR assignment and secondary structure of recombinant RGD-hirudin, Magn. Reson. Chem. 43 (2005) 956–961.
[3] M. Nilges, Calculation of protein structures with ambiguous distance restraints. Automated assignment of ambiguous NOE crosspeaks and disulphide connectivities, J. Mol. Biol. 245 (1995) 645–660.
[4] S.B. Nabburs, C.A.E.M. Spronk, G. Vriend, G.W. Vuister, Concepts and tools for NMR restraint analysis and validation, Concepts Mag. Reson. A 22 (2004) 90–105.
[5] J.P. Linge, M. Nilges, Influence of non-bonded parameters on the quality of NMR structures: a new force field for NMR structure calculation, J. Biomol. NMR 13 (1999) 51–59.
[6] M. Habeck, W. Rieping, J.P. Linge, M. Nilges, NOE assignment with ARIA 2.0: the nuts and bolts, Meth. Mol. Biol. 278 (2004) 379–402.
[7] J.P. Linge, M. Habeck, W. Rieping, M. Nilges, ARIA: automated NOE assignment and NMR structure calculation, Bioinformatics 19 (2003) 315–316.
[8] A.T. Brünger, P.D. Adams, G.M. Clore, P. Gros, R.W. Grosse-Kunstleve, J.S. Jiang, J. Kuszewski, M. Nilges, N.S. Pannu, R.J. Read, L.M. Rice, T. Simonson, G.L. Warren, Crystallography & NMR System: a new software suite for macromolecular structure determination, Acta Crystallogr., D: Biol. Crystallogr. 54 (1998) 905–921.
[9] P.J.M. Folkers, G.M. Clore, P.C. Driscoll, J. Dodt, S. Kohler, A.M. Gronenborn, Solution structure of recombinant hirudin and the Lys-47→Glu mutant: a nuclear magnetic resonance and hybrid distance geometry-dynamical simulated annealing study, Biochemistry 28 (1989) 2601–2617.
[10] T.J. Rydel, A. Tulinsky, W. Bode, R. Huber, Refined structure of the hirudin-thrombin complex, J. Mol. Biol. 221 (1991) 583–601.
[11] G. Wagner, W. Braun, T.F. Havel, T. Schaumann, N. Go, K. Wüthrich, Protein structures in solution by nuclear magnetic resonance and distance geometry: The polypeptide fold of the basic pancreatic trypsin inhibitor determined using two different algorithms, DISGEO and DISMAN, J. Mol. Biol. 196 (1987) 611–639.
[12] M.P. Williamson, T.F. Havel, K. Wüthrich, Solution conformation of proteinase inhibitor II A from bull seminal plasma by I H nuclear magnetic resonance and distance geometry, J. Mol. Biol. 182 (1985) 295–315.
[13] A. Pardi, M. Billeter, K. Wüthrich, Calibration of the angular dependence of the amide proton-C^{α} proton coupling constants, $^{3}J_{HN\alpha}$, in a globular protein: Use of $^{3}J_{HN\alpha}$ for identification of helical secondary structure, J. Mol. Biol. 180 (1984) 741–751.
[14] R. Koradi, M. Billeter, K. Wuthrich, MOLMOL: A program for display and analysis of macromolecular structures, J. Mol. Graph. 14 (1996) 51–55.
[15] R.A. Laskowski, M.W. Macarthur, D.S. Moss, J.M. Thornton, PROCHECK: a program to check the stereochemical quality of protein structures, J. Appl. Crystallogr. 26 (1993) 283–291.
[16] R.A. Laskowski, J.A. Rullmannn, M.W. MacArthur, R. Kaptein, J.M. Thornton, AQUA and PROCHECK-NMR: programs for checking the quality of protein structures solved by NMR, J. Biomol. NMR 8 (1996) 477–486.
[17] D.K. Sukumaran, G.M. Clore, A. Preuss, J. Zarbock, A.M. Gronenborn, Proton nuclear magnetic resonance study of hirudin: resonance assignment and secondary structure, Biochemistry 26 (1987) 333–338.
[18] G.M. Clore, D.K. Sukumaran, M. Nilges, J. Zarbock, A.M. Gronenborn, The conformations of hirudin in solution: a study using nuclear magnetic resonance, distance geometry and restrained molecular dynamics, EMBO J. 6 (1987) 529–537.

[19] H. Haruyama, K. Wüthrich, Conformation of recombinant desulfatohirudin in aqueous solution determined by Nuclear Magnetic Resonance, Biochemistry 28 (1989) 4301–4312.
[20] T. Szyperski, P. Guntert, S.R. Stone, K. Wüthrich, Nuclear magnetic resonance solution structure of hirudin (1–51) and comparison with corresponding three-dimensional structures determined using the complete 65-residue hirudin polypeptide chain, J. Mol. Biol. 228 (1992) 1193–1205.
[21] T. Szyperski, P. Guntert, S.R. Stone, A. Tulinsky, W. Bode, R. Huber, K. Wüthrich, Impact of protein–protein contacts on the conformation of thrombin-bound hirudin studied by comparison with the nuclear magnetic resonance solution structure of hirudin (1-51), J. Mol. Biol. 228 (1992) 1206–1211.
[22] M.G. Grutter, J.P. Priestle, J. Rahuel, H. Grossenbacher, W. Bode, J. Hofsteenge, S.R. Stone, Crystal structure of the thrombin–hirudin complex: a novel mode of serine protease inhibition, EMBO J. 9 (1990) 2361–2365.
[23] W. Bode, I. Mayr, U. Baumann, R. Huber, S.R. Stone, J. Hofsteenge, The refined 1.9 Å crystal structure of human alpha-thrombin interaction with D-Phe-Pro-Arg chloromethylketone and significance of the Tyr-Pro-Pro-Trp insertion segment, EMBO J. 8 (1989) 2361–2365.